

GLUON CHAINS AND MULTIQUARK HADRONS

BY S. JADACH AND M. JEŻABEK

Institute of Physics, Jagellonian University, Cracow*

(Received January 25, 1979)

A monopole approximation to the confining potential is proposed. In this approximation spatially separated groups of quarks carry a definite total colour charge. The potentials which lead to the formation of gluon chains are discussed. The generalization of a $(3, \bar{3})$ chain notion, studied by Tiktopoulos, to the case of arbitrary colour charges is given. It is argued that these generalized chains may be unstable with respect to splitting into a system of weakly interacting chains of the $(3, 3)$ type. A unified picture of the high energy hadronic collisions, based on the gluon chain notion and the monopole approximation is proposed. In the meson-meson sector this picture is equivalent to the topological approach. For the other processes it is similar to the approach of Rossi and Veneziano. However, it is argued that the introduction of the junction line into the quark frame is superfluous. The results are expressed in the language of the coloured dual diagrams which provide a generalization of those of Harari and Rosner.

1. Introduction

In the last few years the growing evidence of the important role played by the colour degree of freedom in the hadronic world has shown the way towards a possible theory of strong interactions. At present, the quantum chromodynamics (QCD) is believed to be the best candidate, although the problem of confinement, i.e. inseparability of quarks, is still not solved [1]. Numerous attempts to applicate QCD for $e^+e^- \rightarrow$ hadrons, deep inelastic lepton-hadron scattering, Drell-Yan pair production, and large p_T processes have been made [2]. On the other hand, the hadronic collisions at low p_T are still "untouchable" in the frame of this theory, because of the above mentioned problem of quark confinement and, consequently, the failure of the perturbative approach. Therefore, one has to look for a phenomenological picture for the medium (~ 1 fm) and long (~ 10 fm) distances. In our opinion this picture should merge our present understanding of the group structure underlying the strong interactions and some "dogmas" discovered in traditional, mainly topological, approaches to the dynamics of hadrons.

The purpose of this paper is to show that a picture of this type may be achieved in the near future. In particular we present a crude and oversimplified model of this type. It relies on the monopole approximation to the confining potential. The idea is that the

* Address: Instytut Fizyki UJ, Reymonta 4, 30-059 Kraków, Poland.

high energy collisions between hadrons which are colour singlets, if looked at in impact parameter space, show that the typical range of the interaction is of order of 1 fm. On the other hand the confining forces have an infinite range. These facts lead to the conjecture that, maybe, the long-range confining forces should be associated with the interaction between colour monopoles, whereas the higher order multipole interactions have the range of order of 1 fm. If this is the case one can easily understand the range of interaction between singlets, because this interaction must be initiated by a non-monopole interaction. If the monopole approximation works, one can show that groups of spatially separated colour charges carry the definite total colours¹ and, consequently, the confining gluonic field has a well-defined colour structure. This leads to the "colour chemistry"², if the energy of the gluon field joining the coloured "atoms" gives the dominant contribution to the total energy of the system. We discuss in more detail the situation when the confining forces are so strong that the vacuum polarization leads to the formation of the so-called gluon chains. However, even if this is not the case, the monopole approximation may still work and, consequently, the colour chemistry also.

The paper is organized as follows: In Section 2 the gluon chain notion is introduced and explored. The idea of the monopole approximation is formulated in a more precise way. The calculation of the asymptotic slopes of the Regge trajectories for multiquark states is presented. At the end of this section the results are compared with those of other models. In Section 3 the unified picture for the high energy collisions between meson-meson, meson-baryon, baryon-baryon, and baryon-antibaryon is presented. It is shown that this picture is equivalent to the dual models in the meson-meson sector, whereas for the other reactions it is very close to the dual approach to baryon dynamics studied recently by Rossi and Veneziano [4]. In particular the new exciting area in the hadron spectroscopy, namely baryonium states, may be studied in the approach which is proposed. However, contrary to the Rossi and Veneziano scheme, in the first approximation all the essential information needed for a description of the high energy processes may be associated with the dynamical degrees of freedom of the valence quarks. Therefore, the incorporation of the new object, the junction line, into the quark model frame may be superfluous. The results are summarized in Section 4, and the calculational methods are described in the Appendix.

2. Gluon chains

2.1. Introductory notes

The gluon chain notion has been introduced by Tiktopoulos [5]. He showed that assuming colour confinement one might get in a non-Abelian gauge theory some configurations of quarks and gluons strongly resembling strings. In particular he has

¹ More precisely, they belong to definite representations of the colour group; projections are not definite, of course.

² This "colour chemistry" assumption is discussed by the Oxford-Rutherford group in the bag model frame [3]. Therefore, the monopole approximation proposed in this paper allows a deeper understanding of the bag model approach, also.

proven that, if the potential binding colour charges is growing faster than linearly with distance, gluons tend to form characteristic configurations between a spatially separated quark and antiquark. His argument based on the variational principle is that the total energy of the system grows only linearly with the length of the chain. These considerations have been generalized to the case when colour charges at the ends of the chain belonged not only to fundamental representations, but also to any higher representation R of the $SU(n_c)$ colour symmetry group [6]. In this section we will discuss an application of the gluon chain notion to the description of highly excited multiquark states, and in the next section to high energy scattering in the zero width limit [4, 11], i.e. for $n_c \gg n_f$, where n_c and n_f denote numbers of colours and flavours, respectively.

2.2. Colour structure of gluon chain

A $(3, \bar{3})$ gluon chain can be described as a system of a quark, k gluons, and an antiquark which form a colourless (singlet) state. The space part of the wave function is built up from nonoverlapping wave packets centered around points $\bar{x}, \bar{z}_1, \dots, \bar{z}_k, \bar{y}$, respectively; these points are ordered along a smooth curve P in space. We consider the configurations for which $|\bar{x} - \bar{y}|$ is large, if compared to a typical size of a hadronic ground state. The colours of quark q , antiquark \bar{q} , and gluons g_r forming the chain are coupled in such a way that, when it is cut at any point in the middle, the total colours of the pieces, $(q, g_1, g_2, \dots, g_i)$ and $(g_{i+1}, \dots, g_k, \bar{q})$, are 3 and $\bar{3}$ respectively, the same as those of q and \bar{q} themselves. Therefore, the colour part of the wave function reads:

$$\psi_{\text{col}} = C_F^{-k/2} (d^{a_1} d^{a_2} \dots d^{a_k})_{\mu\nu}, \quad (2.1)$$

where a_r, μ, ν are the colour indices of the r -th gluon, the quark, and the antiquark respectively. $d_{\mu\nu}^a$ is the matrix element of the a -th generator in the fundamental representation, and it is proportional to the Clebsch–Gordan coefficient $F \otimes A \rightarrow F$ (F denotes the fundamental and A the adjoint representation). C_F denotes the value of the quadratic Casimir operator in the fundamental representation of the gauge group. The colour factor ψ_{col} is also visualized in a pictorial way in Fig. 1. A generalization of the above construction to the case of colour charges R and \bar{R} at the ends of a chain (we call this configuration an (R, \bar{R}) chain) is straightforward. We have to find $X_{\mu\nu}^a$, the matrix elements of the group generators in the representation R , and write

$$\psi_{\text{col}} = M (X^{a_1} \dots X^{a_k})_{\mu_R \nu_R}, \quad (2.2)$$

(see also Fig. 2). It turns out that the normalization factor M is equal to $C_R^{-k/2}$, where C_R denotes the value of the quadratic Casimir operator in the representation R (cf. Appendix). The indices μ_R and ν_R in Eq. (2.2) number states forming the basis of the representation R . Generally, a chain of the (R, \bar{R}) type may split into two chains: (R_1, \bar{R}_1) and (R_2, \bar{R}_2) . In this case we put the corresponding Clebsch–Gordan coefficient $R_1 \otimes R_2 \rightarrow R$ into the colour factor in the junction place. A situation like this occurs, for instance, when we consider the system of two quarks at the end of the chain. Before we start to add to them the colour of the nearest gluon, we couple their colours with the aid of the $F \otimes F \rightarrow R$

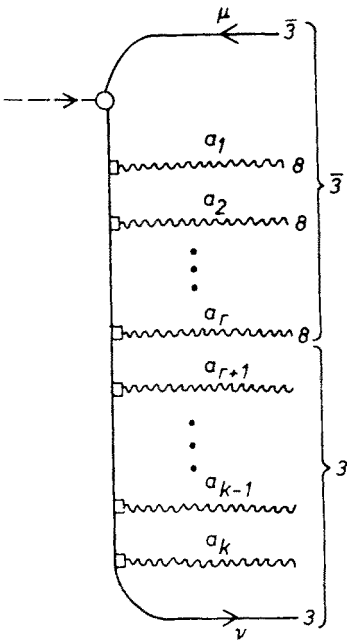


Fig. 1

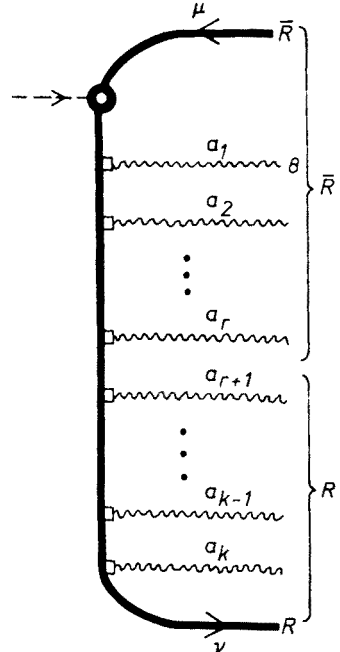


Fig. 2

Fig. 1. The colour structure of the wave function for a $(3, \bar{3})$ chain. The elements of d -matrices are represented by vertices and summation is performed over indices of internal lines. The system is a manifest colour singlet, as it is indicated by the singlet $3\text{--}\bar{3}$ Clebsch–Gordan coefficient represented by a circle

Fig. 2. The colour structure of an (R, \bar{R}) chain. An index μ_R numbers states in the basis of the representation R

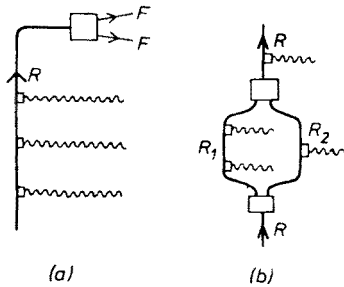


Fig. 3. Examples of junctions: a) the end of the (R, \bar{R}) -type chain connected to two quarks of the total colour R , b) split of the (R, \bar{R}) chain into two chains of the (R_1, \bar{R}_1) and (R_2, \bar{R}_2) type. The boxes are Clebsch–Gordan coefficients projecting $F \otimes F$ onto R and $R_1 \otimes R_2$ onto R , respectively

Clebsch–Gordan coefficients (see Fig. 3a), so, finally we get the colour R at the end of the chain. A similar split may occur also in the middle of the chain (Fig. 3b).

A particular example of the junctions which we discuss here is that joining three dual strings [4] or three $(3, \bar{3})$ chains [5] in the construction of the baryon wave function. Let us notice that gluons in the chain are always coupled to the rest of the chain through

$R \otimes A \rightarrow R$ Clebsch–Gordan coefficients, as is suggested by the interpretation of the chain in terms of the expansion of the multilocal gauge invariant operators³ [5, 4].

We follow Tiktopoulos [5] and neglect velocity and spin dependent terms in the interaction. To describe the interaction between the r -th and s -th packet of the colour charge R and \bar{R} respectively, we choose the following form of the potential:

$$v_{rs} = v(|x_r - x_s|) \sum_a X_{(r)}^a X_{(s)}^a = v(|x_r - x_s|) \hat{v}_{rs} \quad (2.3)$$

In particular we take this form of the potential for the interaction between the ends of the chain. Let us clarify the physical sense of this assumption. The potential (2.3) describes the interaction between two colour monopoles. At this stage we do not consider higher order multipole interactions between the ends of the chain. In other words, the gluon being exchanged between spatially separated packets does not “see” details inside a packet. It sees the total colour, only. Of course, in the future the complete multipole expansion of the potential should be done. This approach may have something to do with the real physical situation when the non-monopole interactions are short-range in the scale of the length of the chain. One may hope that this condition may be fulfilled, because the range of interaction between singlets is of the order of 1 fm, and this interaction is initiated by a non-monopole transition [7]. In that case transitions between chains of different types are suppressed which makes the following scheme self-consistent. A very interesting feature of a gluon chain is the screening of the binding potential v_{rs} . As it has been noted in Ref. [5], the colour part of the matrix element

$$U_{rs} = \langle \psi | v_{rs} | \psi \rangle$$

is damping exponentially the interaction of gluons and/or quarks which have distant positions in the chain

$$U_{rs}^{\text{col}} = \langle \psi_{\text{col}} | \hat{v}_{rs} | \psi_{\text{col}} \rangle \sim \varrho^{|r-s|}, \quad |\varrho| < 1. \quad (2.4)$$

More explicitly, the colour factor for the interaction between the r -th and s -th gluon packets is given by:

$$U_{rs}^{\text{col}} = -C_R^{-k} f_{a_s a_s'}^b f_{a_r a_r'}^b \text{Tr} (X^{a_1} \dots X^{a_r} \dots X^{a_s} \dots X^{a_k} X^{a_k} \dots X^{a_s'} \dots X^{a_r'} \dots X^{a_1}), \quad (2.5)$$

where a summation over repeated indices should be performed, f_{bc}^a are structure constants, and X^a 's are generators in the representation R . This factor is calculated in the Appendix. The result is equal (neglecting a constant which may be absorbed into the space part $v(|x_r - x_s|)$ to $(1 - \varrho_R) \varrho_R^{|r-s|-1}$, where $\varrho_R = 1 - C_A/2C_R$, so, it depends on the ratio C_A/C_R of the quadratic Casimir operators for the adjoint and R -th representation, only. Similarly, the interaction between gluons and colours at the ends of the chain is screened according to (2.4) (see Appendix). The values of ϱ_R for a few of the lowest representations of $SU(3)$ are given in Table I.

³ E. g. the colour structure of a $(3, \bar{3})$ chain may be suggested by the expansion of $O_{M_2} = \bar{q}_i(x_1')$
 $\exp \left[\int_{P(x_1, x_2)} dx^\mu A_\mu \right] q^j(x_2)$.

If the screening is sufficiently effective, the nearest neighbours' interaction will be a good approximation and, consequently, the total potential energy of the system will be proportional to the length of the chain. For more detailed estimations the space part

TABLE I

The dependence of $Q_\beta(R)$ on the potential and on the representation of SU(3) colour

R	C_R	ϱ	Q_1	Q_2	Q_3
3	4	$-\frac{1}{8}$	$\frac{8}{9}$	$\frac{5}{8}\frac{6}{1}$	0.362
6	10	$\frac{11}{20}$	$\frac{20}{9}$	$\frac{62}{8}\frac{0}{1}$	38.4
8	9	$\frac{1}{2}$	2	6	25
10	18	$\frac{3}{4}$	4	28	292

of the wave function is needed, and we return to this problem in the next paragraph. Let us consider now interactions within a system of parallel chains coupled at the ends. As an example let us take the system pictured in Fig. 4a, i.e. two parallel $(3, \bar{3})$ chains joining the spatially separated charges 6 and $\bar{6}$. In this case we have to take into account the interactions between colour charges from different chains as well as those between

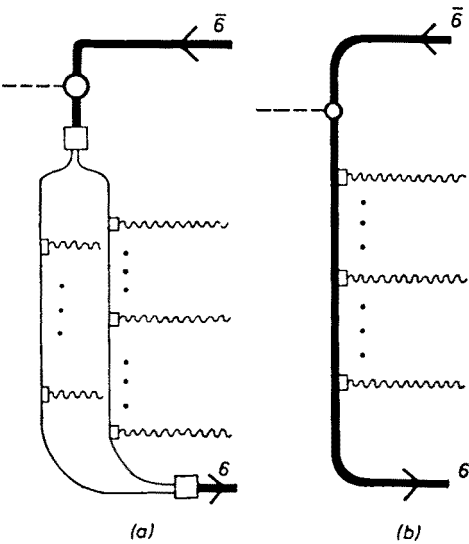


Fig. 4. Two ways of joining separated 6 and $\bar{6}$ colour charges: a) with two $(3, \bar{3})$ chains, and b) with single $(6, \bar{6})$ chain

charges from the same chain. However, it is shown in the Appendix that for long chains the interactions between charges from different chains are negligible. The same result has been obtained for a pair of long $(3, \bar{3})$ chains coupled to 8 and $\bar{8}$ at the common ends, and also for a system of three long $(3, \bar{3})$ chains joining 10 and $\bar{10}$ colour charges.

2.3. Slope of the leading Regge trajectory for exotic states

In order to estimate the slope of the Regge trajectory for the (R, \bar{R}) chain, we follow the ideas of Ref. [8] and minimize the energy of the system at fixed angular momentum. The colour structure of the trial wave function is described in the preceding paragraph. We choose its space part in this way that the resulting Regge trajectory is linear. However, there is still some freedom in the choice of details of the trial function. We carried over calculations for a few different trial functions and the general lesson was the same as that arising from the following simple example. The space part of the wave function of the chain is a product of wave functions for individual links

$$\psi_{\text{spat}} = \Phi_R \left(\prod_{r=1}^k \psi_{\text{spat}}^r(x_r) \right) \Phi_{\bar{R}}. \quad (2.6)$$

Φ_R and $\Phi_{\bar{R}}$ denote wave functions for colour charges R and \bar{R} at the ends of the chain. The gluon packets are centered around points which are placed at equal distances along z axis, i.e. the position of the r -th center is given by

$$\bar{z}_r = 2d(2r - k - 1).$$

The average momentum of the r -th packet is equal to

$$q_r = \left(0, \frac{q}{k-1} (2r - k - 1), 0 \right).$$

We are considering highly excited states; therefore, the number k of gluon packets is large and we neglect the contributions from the ends of the chain in the total energy and angular momentum of the system. If the binding potential is growing as a power of the distance, i.e. $v(r) \sim r^\beta (\beta > 1)^4$, in the large k limit one obtains

$$U \approx \sum_{k \geq s > r \geq 1} U_{rs} \approx A k d^\beta Q_\beta(R). \quad (2.7)$$

For the packets placed at equal distances, a factor $Q_\beta(R)$ may be estimated from the formula

$$Q_\beta(R) \approx (1 - \varrho_R) \sum_{i=1}^{\infty} i^\beta \varrho_R^{i-1}. \quad (2.8)$$

The values of $Q_\beta(R)$ for a few integer powers and lowest dimension representations of $SU(3)$ are displayed in Table I. The "kinetic" part of the energy is obtained as an "uncertainty principle" kinetic energy [5, 9], and the angular momentum of the system is estimated as being equal to

$$J = \sqrt{\sum_{r=1}^k \langle \hat{J}_r^2 \rangle}. \quad (2.9)$$

⁴ We assume that this parametrization holds in the region where the balance between the confining forces and kinetic term of the energy (see text) occurs. The Coulombic-like term ($\sim 1/r$) of the potential may be absorbed e. g. into the kinetic part of the energy. This changes the values of trajectory slopes, but not the ratios which we estimate.

To proceed further, we specify the shape of the gluon packet

$$\psi_{\text{spat}}^r = \pi^{-\frac{3}{2}} d^{-\frac{3}{2}} \exp \left\{ - \frac{x_r^2 + y_r^2 + (z_r - \bar{z}_r)^2}{2d^2} + i q_r y \right\}. \tag{2.10}$$

Now, in the large k limit one can obtain

$$T \approx k \frac{1}{d} \sqrt{\frac{3}{3} + \frac{(qd)^2}{4}}, \tag{2.11}$$

$$J \approx \frac{1}{3} q d k^2. \tag{2.12}$$

Finally, one gets the following expression for the total energy:

$$E = \sqrt{\frac{3J}{qd}} \left[\frac{1}{d} \left(\frac{3}{2} + \frac{(qd)^2}{4} \right)^{\frac{1}{2}} + A Q_\beta d^\beta \right], \tag{2.13}$$

and, after minimization at fixed J , the slope of the Regge trajectory

$$\alpha'_R = \frac{J}{E_{\min}^2} = \text{const} (A, \beta) Q_\beta^{-\frac{2}{\beta+1}}. \tag{2.14}$$

Using this method, we cannot calculate the absolute values of α'_R . We take α'_3 from an experiment, and present the values of α'_R for a few β 's and R 's in Table II. We can now

TABLE II

The Regge trajectory slopes for the multiquark states. We take the experimental value for the (3, 3) trajectory, i. e. $\alpha'_3 = 1 \text{ GeV}^{-2}$

β	1	2	3
α'_3	1	1.00	1.00
α'_6	$\frac{2}{5}$	0.201	0.097
α'_8	$\frac{4}{9}$	0.237	0.120
α'_{10}	$\frac{2}{9}$	0.084	0.035

ask, whether it is possible to build up a trial wave function which is “better”, in the variational method sense, than that which we have considered, i.e. which makes the total energy smaller with angular momentum fixed. Let us take for example two spatially separated colour charges 6 and $\bar{6}$. These two charges may be joined by a single (6, $\bar{6}$) chain (Fig. 4b), but the system of two parallel (3, $\bar{3}$) chains of Fig. 4a should also be taken into consideration. Eqs. (2.7), (2.11) and (2.12) suggest that the latter configuration makes the mean value of the hamiltonian smaller than the former one does in the case when $\alpha'_3 > 2\alpha'_6$ and intercepts of the trajectories can be neglected. Thus, for highly excited states and the β 's displayed in Table II, we can expect that the double-chain structure of Fig. 4a provides a better approximation to the “true” wave function than a single

(6, $\bar{6}$) chain. This result arises from the screening of the interaction between parallel chains, the fact which we have discussed in the preceding paragraph. A similar conclusion can be drawn for a system of separated 8 and $\bar{8}$ charges, and also for a 10— $\bar{10}$ pair, which may split into three parallel chains. Thus, we expect that asymptotically $\alpha'_6 \approx \alpha'_8 \approx \frac{1}{2}$ and $\alpha'_{10} \approx \frac{1}{3}$.

2.4. Gluon chain picture vs dual models and MIT bag model

The gluon chain picture seems to be closely related to the dual models [10, 11, 4] and string models [12–14]. The concept of the chain is also suggested by the path dependent gauge-invariant bilocal operator $O_{M_2}(P)$ of a quark-antiquark pair (c.f. Fig. 5). On the other hand the correspondence between the irreducible gauge-invariant operators⁵ and

Hadron	Gauge invariant operator	String picture
$M_2 = q\bar{q}$ meson	$\bar{q}(x_1) \exp \left(g \int_{x_1}^{x_2} dx_\mu A^\mu \right) q(x_2)$	
$M_0 = \text{quarkless meson}$	$\text{Tr} \exp \left(g \oint dx_\mu A^\mu \right)$	
$B_3 = qq\bar{q}$ baryon	$\epsilon_{ijk} \left[\exp \left(g \int_{x_1}^{x_2} dx_\mu A^\mu \right) q(x_1) \right]_i \times \left[\exp \left(g \int_{x_2}^{x_3} dx_\mu A^\mu \right) q(x_2) \right]_j \left[\exp \left(g \int_{x_3}^{x_1} dx_\mu A^\mu \right) q(x_3) \right]_k$	
$M_6^J = \text{baryonium with } qq\bar{q}\bar{q} \text{ QN}$	$\epsilon_{ijk} \epsilon_{i'j'k'} \left[\bar{q} \exp \left(\int_{x_1}^{y_1} \right) \right]_i \left[\bar{q} \exp \left(\int_{x_2}^{y_2} \right) \right]_j \times \left[\exp \left(\int_{x_1}^{y_1} \right) q \right]_{k'} \left[\exp \left(\int_{x_2}^{y_2} \right) q \right]_{j'}$	
$M_2^J = \text{baryonium with } q\bar{q} \text{ QN}$	$\epsilon_{ijk} \epsilon_{i'j'k'} \left[\bar{q} \exp \left(\int_{x_1}^{y_1} \right) \right]_i \times \left[\exp \left(\int_{x_1}^{y_1} \right) q \right]_{k'} \left[\exp \left(\int_{x_2}^{y_2} \right) q \right]_{j'}$	
$M_0^J = \text{quarkless baryonium}$	$\epsilon_{ijk} \epsilon_{i'j'k'} \times \left[\exp \left(\int_{x_1}^{y_1} \right) \right]_{j'} \left[\exp \left(\int_{x_2}^{y_2} \right) \right]_{k'} \left[\exp \left(\int_{x_3}^{y_3} \right) \right]_{k'}$	

Fig. 5. Examples of the correspondence principle between irreducible gauge-invariant operators and dual-string states (from Veneziano, Ref. [15])

dual strings has been argued many times [15] (see also Fig. 5). For multiquark states the split of (R, \bar{R}) chains might provide an explanation of the weak interaction between strings, assumed in the string picture. However, this split does not occur for low mass excitations. In that regime a description based on e.g. the MIT bag model [16, 17] seems to be more appropriate.

An interesting example is that of the $\psi(700)$ state. This particle has been interpreted in the MIT bag model as a member of a 0^{++} nonet composed of $qq\bar{q}\bar{q}$ states [17]. The

⁵ In terminology of Ref. [15] a colour singlet operator is irreducible if it cannot be represented by a product of two non-trivial colour singlet operators.

recent phenomenological analysis of Holmgren and Pennington [18] confirms this conjecture. Furthermore, their results suggest that this state is a mixture of M_4^J baryonium and a system of two M_2 mesons⁶ with significant contributions of all these states. Therefore, the usefulness of the dual classification [4, 15] for ground states of multi-quark systems may be put in doubt.

The MIT bag model's version for highly excited states has also been studied [8, 19–21] and its consequences are in disagreement with the expectations of dual models and the gluon chain model. However, one may argue that the universal pressure approximation which works surprisingly well for ground hadronic states may fail in the presence of vacuum polarization effects which produce a gluon chain between distant colour charges.

3. Gluon chains and the unified dual approach to the dynamics of hadrons

In this section we argue that the monopole approximation to the confining potential (cf. Eq. (2.3)) leads to the unified description of meson-meson, meson-baryon, baryon-baryon, and baryon-antibaryon processes at high energies. It is shown that the colour plays an essential role in solving some old puzzles which appear in the dual quark models when the colour degrees of freedom are not taken into consideration. In fact this point is not new. This idea has been formulated and fully explored in the paper of Rossi and Veneziano [4]. The approach which we propose follows step by step that of Ref. [4]. The phenomenological consequences are almost the same, with one exception which we comment on further. However, we point out that the results of Ref. [4] may be reproduced without the introduction of a new “being”, the junction line. Instead, we explore the fact that in the high energy processes some groups of coloured constituents of the colliding hadrons may carry a definite colour. This happens when the monopole approximation works well.

We introduce also coloured dual diagrams and formulate our results in their language. The strict correspondence between coloured dual diagrams and those of Harari and Rosner [22] exists in the meson-meson sector. However, for more complicated systems of quarks one has to indicate what is the total colour of the system. For this purpose we introduce colour lines which are associated with groups of quark lines. We argue also that these diagrams which are built up (in the s -channel unitarity sense) from the s -channel intermediate states containing hard valence gluons, should be suppressed and considered as corrections which emerge in the unitarization procedure. In this way we detach the set of “allowed” diagrams which (with a single exception) is the same as that considered in the dual approach to baryons [4]. This result seems to be of some importance, because it means that a consequent dynamical scheme for baryons may be obtained, which in the first approximation appeals to the valence quarks only. Therefore, nice correspondence is achieved with the old “uncoloured” quark models. In the Rossi–Veneziano scheme one has to consider the junction, an object which is conceptually new from the quark model point of view. This object carries very essential dynamical information, and it means that

⁶ We use the terminology of Fig. 5 and Ref. [15].

the quark model builders have to find some way to incorporate this new "being" into their schemes. What follows from our scheme means that this effort may be superfluous. The arguments which we present below hold in the zero width limit, i. e. for $n_c \gg n_f$ (cf. paragraph 2.1). It is shown in Ref. [4] in what way one can introduce quark loops and other higher order corrections into the unitarization procedure. The results of the unitarization for our scheme are nearly the same as those of Ref. [4], because of the above mentioned similarity between the starting points. Therefore, we skip the detailed discussion of the phenomenological consequences for which we refer to the original paper of Rossi and Veneziano. However, let us note briefly the consequence which seems to be very interesting. There is a possibility that different colour configurations may lead to different jet structures. We have shown that, because of the splitting of chains, the triplet-antitriplet system may be accompanied by a single $(3, \bar{3})$ chain, whereas $6-\bar{6}$ and $8-\bar{8}$ by two $(3, \bar{3})$

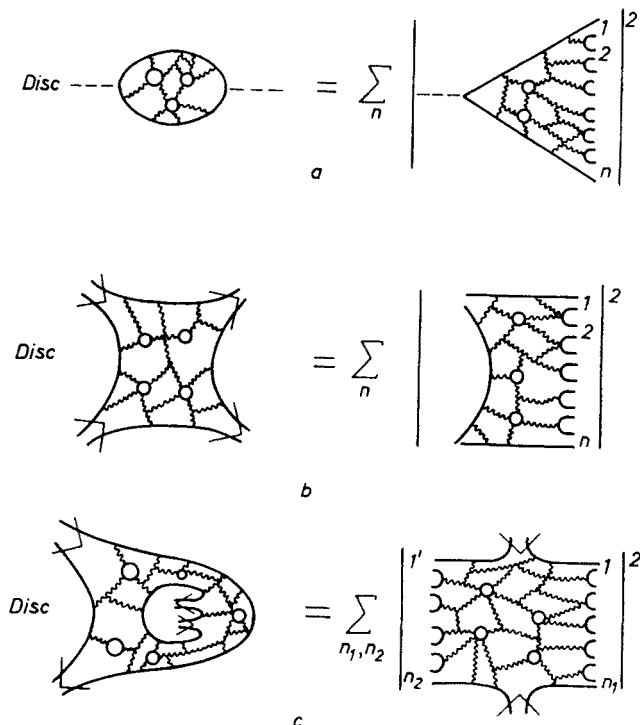


Fig. 6. a) $1/n$ expansion for $\sigma_{\text{tot}}(e^+e^- \rightarrow \text{hadrons})$; b) s -channel content of the bare reggeon; c) s -channel content of the bare Pomeron

chains, and $10-\bar{10}$ even by a system of three gluon chains of the $(3, \bar{3})$ type. After inclusion of quark loops these different structures may lead to one-, two-, and three-jet structures respectively. It has been shown [23, 24] that there exist some promising methods of studying the jet structures. So, in some sense, we may "see" the colour even in the "normal" low p_T processes.

Let us consider now two-body scattering of hadrons at high energies. Through the s -channel unitarity, the absorptive part of the amplitude may be related to the cross-sections for the production of the intermediate states obtained by an s -channel cut of the corresponding dual diagram. The examples of this procedure are shown in Fig. 6a-c. If $\varrho = n_t/n_c$ is small, the corrections due to the quark line insertions may be neglected. Thus, it is preferable to consider an s -channel picture of long-living compounds (cf. Fig. 7a-d) which for large s are identified with gluon chains.⁷ The type of the chain in

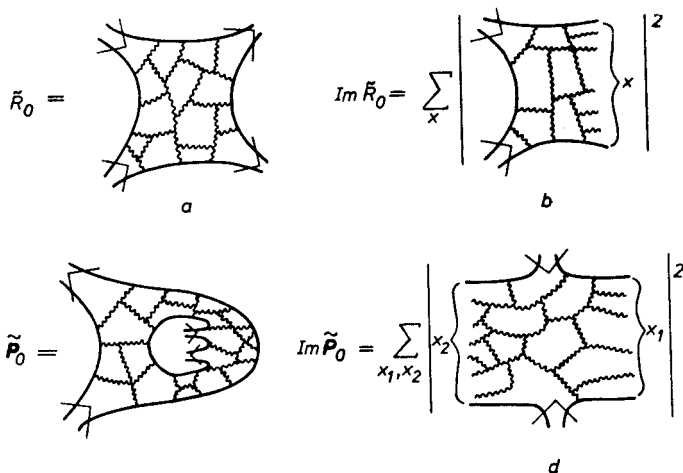


Fig. 7. Leading terms in $1/n_c$ expansion of QCD: a) the bare reggeon, b) s -channel content of the bare reggeon, c) the bare Pomeron, and d) s -channel content of the bare Pomeron

a specific reaction is related to the colour of the valence constituents of scattered hadrons. Therefore, correspondence is obtained between this approach and those “old” schemes which do not take the colour into account when one assumes that only a valence quark may belong to the set of valence constituents of hadrons. In parton language it means that there are no hard gluons inside hadrons (the distribution of gluons, $g(x)$, vanishes rapidly for the Feynman x near 1). In that case the fact that violations of OZI rule seem to be very small for large masses (asymptotic planarity [10]) may be easily understood as a consequence of momentum conservation.

Let us now introduce the set of diagrams, analogous to that of Harari and Rosner [22], which take the colours of quarks into account. Let the full line running from the left to the right (Fig. 8a) represents a quark, and that oriented in the opposite direction an anti-quark (Fig. 8b). To describe collisions between mesons, baryons, and antibaryons one needs graphical symbols for the colour group representations up to 10-dimensional.

⁷ The s -channel intermediate states are grouped along the peripheral curve ($M \sim J$) in the Chew-Frautschi plane. The gluon chain for that case looks similarly to that discussed in the preceding section. The only difference is that the angular momenta of packets need not be parallel as they do in the leading trajectory case.

However, one may reduce a number of new elements to three with the aid of the convention that, if there is no special colour line associated with the system of full (quark and/or antiquark) lines, the total colour of the system is the smallest obtained from coupling colours carried by these lines. So, for instance, the system of two quark lines with no special

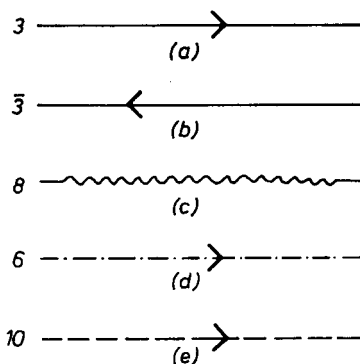


Fig. 8. Coloured dual diagrams: special colour lines for a) triplet, b) antitriplet, c) octet, d) sextet, and e) decuplet. The reversion of an arrow gives the state in the conjugate representation

indication of the colour has a total colour anti-three. It may happen that the colour associated with a system of quark lines cannot be obtained by coupling the “visible” colours. This reflects the contribution from gluons in the total colour of the system. The new elements, which we have to introduce, are colour lines denoting a flow of the colour 8, 6, and 10 respectively (Fig. 8c-e). The orientation of lines is significant; the reversion

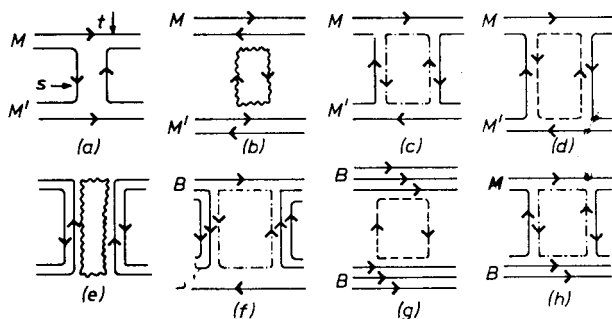


Fig. 9. Coloured dual diagrams: examples. Allowed diagrams for meson-meson: a) reggeon exchange, b) Pomeron exchange, and c-e) forbidden diagrams. Examples of forbidden diagrams for f) baryon-anti-baryon, g) baryon-baryon, and h) meson-baryon scattering

of an arrow gives a conjugate representation. Let us consider now the meson-meson elastic scattering and identify the terms in the $1/n_c$ expansion (cf. [9, 11, and 4]) with the coloured diagrams introduced above. The diagram of Fig. 9a may be easily assigned to the bare reggeon. It follows from the relation between $(3, \bar{3})$ chain and gauge invariant operators O_{M_2} (cf. Fig. 5). The situation is more complicated for the diagrams depicted in Fig. 9b.

The s -channel cut leads to the system of two octets (Fig. 10a) which may be joined by an $(8, \bar{8})$ chain.

As it has been pointed out, the $(8, \bar{8})$ chain splits into two chains of the $(3, \bar{3})$ type (Fig. 10b). This is exactly what we need to establish the connection with the bare Pomeron in the $1/n_c$ expansion. However, the colour charge 8 may be completely screened by a system of gluons. So, the configuration of Fig. 10c should be also taken into account.

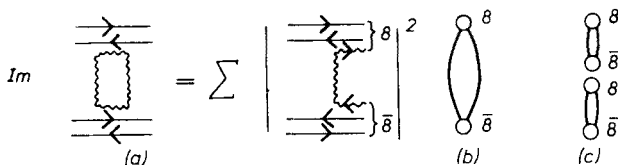


Fig. 10. a) the s -channel structure of diagram 9b, b) system of octet-anti-octet joined with two $(3, \bar{3})$ chains, and c) a colour structure for diffractive excitations

There are some phenomenological suggestions that states like this may have something to do with diffractive excitations [25]. In the topological approach, on the other hand, one can show that contributions from configurations of this type are damped by a factor $1/n_c^2$ with respect to the leading double string term. So, we associate a split $(8, \bar{8})$ chain (Fig. 10b) with the bare Pomeron. The diagrams pictured in Figs. 9c–e are all suppressed in the topological approach, and they are considered as higher order corrections in the unitarization procedure. One can see that all these diagrams are “built up” from the intermediate states containing the valence gluons. So, probably the coupling of “ordinary” hadrons to those with valence gluons is small. If this is the case, we can extract the following rules for drawing the coloured dual diagrams:

- a) each quark and colour line retains its identity,
- b) diagrams with valence gluons in the s -channel intermediate states are suppressed.

With the aid of these rules one can easily draw dual diagrams for meson-meson, meson-baryon, baryon-baryon, and baryon-antibaryon scattering. The leading contributions are depicted in Fig. 11. For a baryon-antibaryon collision one-, two-, and three-jet annihilation appears. A reggeon exchange in $B\bar{B}$ is dual to the diquark-antidiquark s -channel configuration. The scheme which emerges is almost identical to the dual approach for baryons of Ref. [4]. However, there is one exception: in the scheme of Rossi and Veneziano the diagram of Fig. 9f is “built up” from M_2^J baryonium states which are strongly coupled to the $B\bar{B}$ channel. In our approach this diagram must be suppressed, because a single quark line cannot carry the colour six. Unfortunately, this difference cannot be used as a starting point for some simple experimental test, because the eventual contribution from the diagram being discussed is masked by the Pomeron and reggeon exchanges.

One may prefer Rossi and Veneziano’s scheme, because of the nice symmetry between M_2^J and M_4^J baryonia in the crossed s and t channels, but one has also to take into account that an “ugly asymmetry” between e. g. diagrams 9a and 9e seems to be commonly accepted. It is noteworthy to stress that the gluon chain picture is less ambitious than the dual approach of Ref. [4]. The former one is bounded to highly excited and asymmetric hadronic

states. These states are described in a way very similar to the “colour chemistry” of Chan Hong-Mo and his co-workers [3]. Coloured constituents of a hadron are divided into a few groups — “atoms”. These groups from the same atom are spatially correlated. Complicated interactions between constituents are hidden inside atom-coloured ends of

Process	Baryon - -baryon	Meson - -meson	Meson - -baryon	Baryon - -antibaryon	Colour structure of s-channel intermed. state
Pomeron (M_0) exchange					
reggeon (M_2) exchange					
M_0^J exchange					
M_2^J exchange					
M_4 exchange					

Fig. 11. Allowed coloured dual diagrams for baryon-baryon, meson-meson, meson-baryon, and baryon-antibaryon

the chain. When a hadron-“molecule” is highly excited the distances between atoms are large. The atoms are kept together by gluon chains, string-like configurations of the gluonic field. We have considered linear configurations only, and we hope that these give the dominant contribution to the dynamics of “ordinary” hadrons, although the rich structure of Y shaped excitations [4] may play an important role in collisions between some “unusual” states. It is obvious that the “chemical” description gets too rough for low mass excitations, and one has to use a more realistic model (maybe the MIT bag model) in this regime.

The beautiful feature of the Rossi-Veneziano approach is that it covers both low and high energy regions, though the predictive power of the model may be lost, if the mixing between states of different types is large for low energies. The recent phenomenological analysis [26] has shown that this is exactly what happens.

To summarize: the model which we propose in many aspects reminds one of the dual models for mesons [10] and for baryons [4]. In particular it helps to understand why the interaction between strings in a multistring system may be small. This phenomenon is explained by a screening of the binding potential, and it is due to the non-Abelian nature

of the colour charges forming a chain. However, it does not mean that this interaction is negligible for every system of chains. This is the interaction between chains which leads to the suppression of M_4 two-meson exchange (Fig. 9f) in our scheme, and consequently, causes its non-equivalence to the approach of Ref. [4] in the high energy regime.

4. Summary

The results of this paper may be summarized in the following way:

The monopole approximation to the confining potential at large (~ 10 fm) distances is proposed and argued. In this approximation spatially separated groups of colour charges carry a definite total colour.

It is shown that some puzzles of those old quark models which do not take the colour into account may be solved, if one considers states with the definite total colour. The coloured dual diagrams, which provide a generalization of those of Harari and Rosner, are introduced.

The gluon chain notion, which has been studied by Tiktopoulos for a quark-antiquark pair, is generalized to the case of arbitrary colour charges. The stability of (R, \bar{R}) chains is studied. It is shown that an (R, \bar{R}) chain may be instable with respect to splitting into the system of weakly interacting $(3, \bar{3})$ chains.

The asymptotic slopes of the Regge trajectories for the exotic multiquark states are estimated.

The unified picture of meson-meson, meson-baryon, baryon-baryon, and baryon-antibaryon high energy collisions is proposed. This picture relies on the monopole approximation, the gluon chain notion, and the zero width limit. As it has been shown by Rossi and Veneziano, the last limitation may be relaxed with the aid of the dual unitarization. In the meson-meson sector the proposed picture seems to be equivalent to the topological approach. For the other processes this picture is very similar to that of Rossi and Veneziano. However, it is shown that the incorporation of the junction line into the quark model frame may be superfluous, because in the first approximation of the unitarization procedure all the essential dynamical information can be related to the valence quark degrees of freedom.

We would like to thank Professor A. Białas and Dr. K. Fiałkowski for their constant help during this work, reading the manuscript, and stimulating discussions. We are indebted to Professor G. F. Chew and Dr. J. Kwieciński for illuminating discussions. We wish also to thank our colleagues at Jagellonian University: W. Furmański, W. Słomiński, J. Szwed, M. Zieliński, and P. Żenczykowski for many helpful remarks.

APPENDIX A

Notation

In calculations of group theory factors we use the following diagrammatic notation [27]:

1) Each external line represents a state in some irreducible representation of the gauge group $SU(3)_{\text{colour}}$. We assign a dashed line to the unit representation, a wavy line to the adjoint representation and solid lines to the fundamental representation F and its

3) The vertex of Fig. A3a denotes a fully antisymmetric coupling of three gluons, and that of Fig. A3b represents a projection of the singlet onto $R \otimes \bar{R}$. Lines circle these vertices in anticlockwise direction. The orientation of solid lines in Fig. A3b is significant: the outward line denotes a state in the defining representation F , and that with reversed arrow a state in \bar{F} . The vertex pictured in Fig. A3c represents a projection of $R \otimes \bar{R}$ onto the singlet. The minus sign indicates a clockwise ordering of lines. The orientation of solid lines is just opposite to that of Fig. A3b.

4) The vertex in Fig. A4a represents the action of a generator on a state in the representation F . The generator is a matrix proportional to the Gell-Mann matrix λ_a . The same

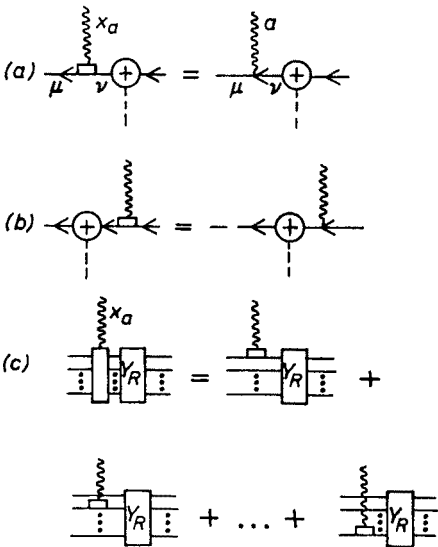


Fig. A4. The action of the generator X_a on a state in a) defining 3 , b) conjugate $\bar{3}$, and c) representation R vertex, but with a minus sign and transposed indices, is used for the complex conjugate representation \bar{F} , Fig. A4b. The rule of Fig. A4c completes the above definition for the remaining representations. It states that the generator acts on a product state as a direct sum of the generators restricted to particular states in the product.

APPENDIX B

A few useful relations

In this section we present in a diagrammatic form some relations which make a calculation of colour factors for gluonic chains easier. In what follows a solid line with the capital R denotes a state in the representation R .

1) The commutation relations for the Lie algebra $[X_a, X_b] = iC_{ab}^c X_c$ are drawn in Fig. B1a–c. The last one can be also understood as the Jacobi identity (Fig. B1c).

2) Graphs which contain $R\text{--}\bar{R}$ -singlet vertices can be simplified with the aid of rules B3a–b.

3) The “black box” formulas of Figs B4a–b are used for the reduction of complex graphs, constructed from the lines and vertices described above. The box containing only index contractions is a scalar. The equalities B4c–e are simple corollaries of the preceding ones.

4) In addition there are two relations depicted in Figs B5a–b which result from B1a, B2a, B2c and A3a, and will be useful in further calculations.

$$\begin{aligned}
 (a) \quad & \text{Diagram 1} - \text{Diagram 2} = \text{Diagram 3} \\
 (b) \quad & \text{Diagram 4} - \text{Diagram 5} = \text{Diagram 6} \\
 (c) \quad & \text{Diagram 7} - \text{Diagram 8} = \text{Diagram 9}
 \end{aligned}$$

Fig. B1. Lie commutator for a) representation R , b) defining representation, and c) adjoint representation

$$\begin{aligned}
 (a) \quad & \text{Diagram 10} = C_R \text{Diagram 11} \\
 (b) \quad & \text{Diagram 12} = C_F \text{Diagram 13} \\
 (c) \quad & \text{Diagram 14} = C_A \text{Diagram 15}
 \end{aligned}$$

Fig. B2. Graphical representation of the quadratic Casimir operator for a) representation R , b) defining representation, and c) adjoint representation

$$\begin{aligned}
 (a) \quad & \text{Diagram 16} = \frac{1}{\dim(R)} \text{Diagram 17} \\
 (b) \quad & \text{Diagram 18} = - \text{Diagram 19}
 \end{aligned}$$

Fig. B3. Properties of the $R \otimes \bar{R}$ singlet vertex: a) elimination of two vertices; $\dim R$ is the dimension of representation, b) invariance of the projection vertex under infinitesimal transformations

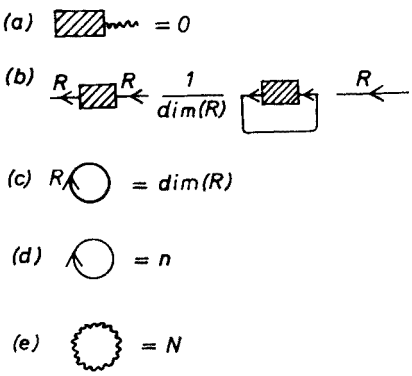


Fig. B4. a) “colour conservation”, b) elimination of a scalar operator, c) dimension of the basis of representation R , d) number of colours, and e) number of gluons

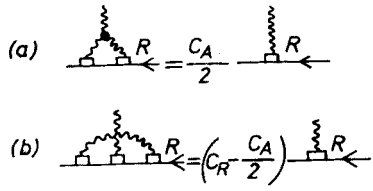


Fig. B5. a-b) Examples of the reduction of $R-\bar{R}$ -octet vertices

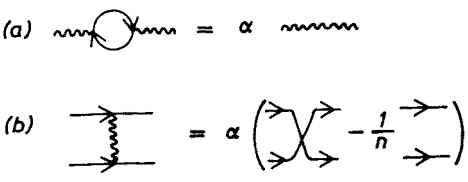


Fig. B6. a) Normalization of the trace of two generators, b) elimination of the quark-gluon vertex

5) The relations of Figs B6a–b are equivalent to

$$\text{Tr} (X_a X_b) = \alpha \delta_{ab}, \tag{B6a}$$

and

$$\sum_{a=1}^8 (X_a)_{ij} (X_a)_{kl} = \alpha \left(\delta_{il} \delta_{kj} - \frac{1}{n} \delta_{ij} \delta_{kl} \right), \tag{B6b}$$

respectively. The normalization factor depends on the choice of generators; e. g. $\alpha = 2$ for $X_a = \lambda_a$.

APPENDIX C

Colour factors for gluon chains

The unnormalized wave function $|\psi_{R,\bar{R}}^{\text{un}}\rangle$ for the (R, \bar{R}) gluon chain is depicted in Fig. 2. As a first exercise we calculate its normalization $M = \langle \psi_{R,\bar{R}}^{\text{un}} | \psi_{R,\bar{R}}^{\text{un}} \rangle$. This is demonstrated in Fig. C1. For k gluon packets the result is $M^{-2} = C_R^k$; and we define $|\psi_{R,\bar{R}}\rangle = M |\psi_{R,\bar{R}}^{\text{un}}\rangle$.

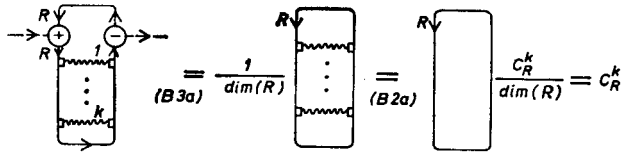


Fig. C1. Normalization of the wave function for the (R, \bar{R}) chain

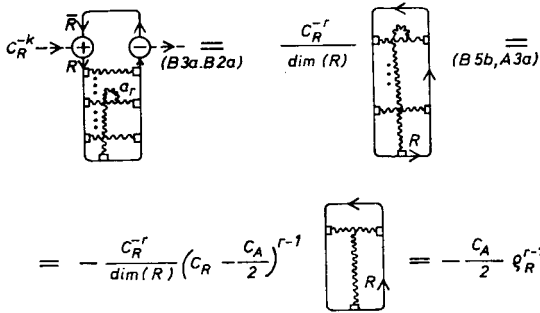


Fig. C2. Colour factor for the interaction between r -th gluon packet and the colour charge R at the end of the chain

Let us now calculate the colour part of the interaction between the r -th packet and “colour charge” R at the end of the chain. It is demonstrated in Fig. C2 that $\langle \psi_{R,\bar{R}} | \hat{v}_{r,R} | \psi_{R,\bar{R}} \rangle$, the matrix element which we need, is equal to $-\frac{C_A}{2} Q_R^{r-1}$. Similarly, for the interaction between this packet and the other end of the chain we get

$$\langle \psi_{R,\bar{R}} | \hat{v}_{\bar{R},r} | \psi_{R,\bar{R}} \rangle = -\frac{C_A}{2} Q_R^{k-r}.$$

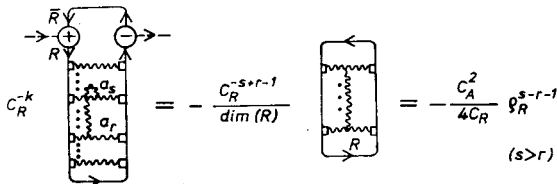


Fig. C3. Colour factor for the interaction between r -th and s -th gluon packet in the (R, \bar{R}) chain

The most important contribution to the potential energy comes from interactions between gluon packets. Garphical calculations, see Fig. C3, give $\langle \psi_{R,\bar{R}} | \hat{v}_{rs} | \psi_{R,\bar{R}} \rangle = -\frac{C_A}{2} (1 - \varrho_R) \varrho_R^{|s-r|-1}$.

Let us now construct the colour part of the wave function for two parallel $(3, \bar{3})$ chains coupled at the ends to colour charges 6 and $\bar{6}$. The unnormalized wave function is shown in Fig. 4a. The symmetrization symbol P projects the $3 \otimes 3$ product onto the six-dimen-

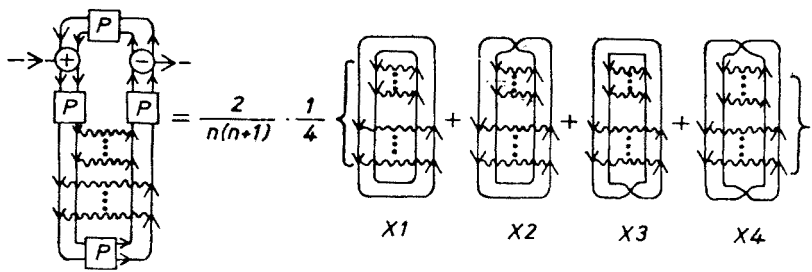


Fig. C4. Normalization of the wave function for two $(3, \bar{3})$ chains coupled to 6 and $\bar{6}$ colour charges

sional representation of the group. In order to calculate the normalization we replace the symmetrization symbol by its definition, see Fig. C4. Now we have to calculate four graphs. The first three of them are trivial: $X1 = n^2 C_F^{k+l}$. $X2 = X3 = n C_F^{k+l}$, where C_F denotes

$$W_r = \text{[Diagram of two loops connected by a vertical line]} = \alpha \left\{ \text{[Diagram of two loops connected by a vertical line with a cross]} - \frac{1}{n} \text{[Diagram of two loops connected by a vertical line with a cross]} \right\}$$

Fig. C5. The recurrence relation for the graph $X4$ in Fig. C4

the quadratic Casimir operator for the fundamental representation, and k and l are the numbers of packets in the chains. The last one, $X4$, can be calculated by repeated use of the relation B6b. The recurrence relation, see Fig. C5, is obtained

$$W_r = \alpha n C_F^{r-1} - \frac{\alpha}{n} W_{r-1} = \frac{C_A}{2} C_F^{r-1} + C_F \varrho_F W_{r-1},$$

where $W_{k+l} = X4$ and $W_1 = 0$. The solution is

$$X4 = C_F^{k+l} (1 - \varrho_F^{k+l-1}) \cong C_F^{k+l},$$

and finally we get the normalization factor:

$$M^{-2} = \frac{1}{2n(n+1)} C_F^{k+l} [(n+1)^2 - \varrho_F^{k+l-1}] \approx \frac{n+1}{2n} C_F^{k+l}.$$

In a similar way one calculates interaction terms. For example the factor $\langle \psi | \hat{v}_{1r,1s} | \psi \rangle$, where the r -th and s -th gluon packets belong to the same chain, is represented by the graph of Fig. C6a. We eliminate symmetrization symbols and get three graphs which

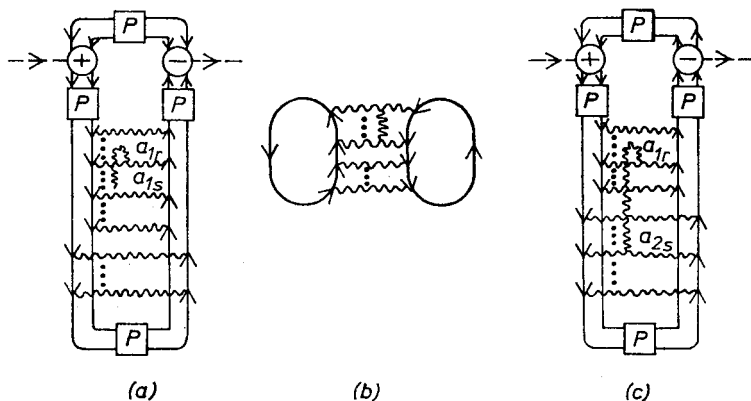


Fig. C6. Colour factors for two $(3, \bar{3})$ chains coupled to 6 and $\bar{6}$ colour charges: a) interaction of two gluon packets from the same chain, b) typical graph, c) interaction of two packets from different chains

can easily be reduced, and a new one depicted in Fig. C6b. We calculate it with the aid of Fig. B6b removing gluon lines one by one. At last we obtain the following result:

$$\langle \psi | \hat{v}_{1r,1s} | \psi \rangle = -\frac{C_A}{2} (1 - \varrho_F) \varrho_F^{|r-s|-1} + O(\varrho_F^{k+l-|r-s|-1}),$$

which is, up to the terms negligible for the long chain, identical to that for the single $(3, \bar{3})$ chain. Very similar calculations with almost the same graphs give the colour factor for interactions between packets from different chains (cf. Fig. C6c):

$$\langle \psi | \hat{v}_{1r,2s} | \psi \rangle = \text{const} [\varrho_F^{r+s-2} + \varrho_F^{k+l-r-s}] + O(\varrho_F^{k+l}),$$

which is damping the interaction exponentially unless both gluon packets are placed near the same junction simultaneously. Moreover, one can check that in the long chain case the interaction of central packets with the charges at the ends is strongly screened just as in a single $(3, \bar{3})$ chain case. Consequently, the only important contribution to the total energy of the system comes from the interactions between gluon packets from the same chain.

REFERENCES

- [1] W. Marciano, H. Pagels, *Phys. Reports* **40C**, No 3 (1978).
- [2] G. Sterman, S. Weinberg, *Phys. Rev. Lett.* **39**, 1436 (1977); W. Furmański, *Large p_T Cross-Sections from Quantum Chromodynamics*, Jagellonian Univ. preprint TPJU-10/78 and references quoted therein; W. Furmański, *Jets from QCD*, Jagellonian Univ. preprint TPJU-11/78.
- [3] H.-M. Chan, Lectures delivered at the XVIII Cracow School of Theoretical Physics, Zakopane (June 1978).
- [4] G. C. Rossi, G. Veneziano, *Nucl. Phys.* **B123**, 507 (1977).

- [5] G. Tiktopoulos, *Phys. Lett.* **66B**, 271 (1976).
- [6] S. Jadach, M. Jeżabek, Jagellonian Univ. preprint TPJU-5/78.
- [7] The consequences of the dipole-dipole forces between hadrons have been studied by P. M. Fishbane, M. T. Grisaru, *Phys. Lett.* **74B**, 98 (1978). Van der Waals-type forces discussed in this paper are short-range, in agreement with our general argument. We are indebted to Dr. K. Fiałkowski who has called our attention to this paper.
- [8] K. Johnson, C. B. Thorn, *Phys. Rev.* **D13**, 1934 (1976).
- [9] G. 't Hooft, *Nucl. Phys.* **B72**, 461 (1974).
- [10] For a review see G. F. Chew, C. Rosenzweig, *Dual Topological Unitarization: an Ordered Approach to Hadron Theory*, to be published in *Phys. Reports* (1978).
- [11] G. Veneziano, *Nucl. Phys.* **B117**, 519 (1976).
- [12] For a review of the dual string model, see *Dual Theory*, Physics Reports Reprint Book Series, Ed. M. Jacob, vol. 1, 1976.
- [13] M. Imachi, S. Otsuki, F. Toyoda, *Prog. Theor. Phys.* **55**, 551 and 1211 (1976); **57**, 517 (1977).
- [14] I. Bars, *Phys. Rev. Lett.* **40**, 688 (1978).
- [15] G. Veneziano, CERN preprint TH-2425 (1977), and references quoted therein.
- [16] For a review, see K. Johnson, *Acta Phys. Pol.* **B6**, 865 (1975); P. Hasenfrantz, J. Kuti, *Phys. Reports* **40C**, No 2 (1978).
- [17] R. L. Jaffe, K. Johnson, *Phys. Lett.* **60B**, 201 (1976); R. L. Jaffe, *Phys. Rev.* **D15**, 267 and 281 (1977).
- [18] S. O. Holmgren, M. R. Pennington, CERN preprint TH. 2464, April 1978.
- [19] H.-M. Chan, H. Hogaasen, *Phys. Lett.* **72B**, 121 (1977); **72B**, 400 (1978).
- [20] M. Fukugita, K. Konishi, T. H. Hansson, *Phys. Lett.* **74B**, 261 (1978).
- [21] H. Hogaasen, P. Sorba, CERN preprint TH. 2500, May 1978.
- [22] H. Harari, *Phys. Rev. Lett.* **22**, 562 (1969); L. Rosner, *Phys. Rev. Lett.* **22**, 689 (1969).
- [23] A. Giovannini, G. Veneziano, CERN preprint TH. 2347, 1977.
- [24] M. Jeżabek, Ph. D. thesis, Jagellonian University, Cracow 1978, and references quoted therein.
- [25] A. Białas, A. Czachor, *Acta Phys. Pol.* **B9**, 341 (1978); A. Białas, A. Czachor, J. Szwed, *Acta Phys. Pol.* **B9**, 875 (1978).
- [26] M. R. Pennington, CERN preprint TH. 2457, 1978, to be published in *Nucl. Phys.*
- [27] For a review of diagrammatic methods in the group theory see e. g.: P. Cvitanovic, *Phys. Rev.* **D14**, 1536 (1976); G. P. Canning, *Diagrammatic Group Theory in Quark Models*, Bonn University preprint, BONN-HE-77-10.